

## Stable p-type ZnO thin films on sapphire and n-type 4H-SiC achieved by controlling oxygen pressure using radical-source laser molecular beam epitaxy

Li Meng<sup>1,2</sup>, Jingwen Zhang\*, Jian An<sup>1,2</sup>, and Xun Hou<sup>1</sup>

Received 26 June 2015, revised 6 September 2015, accepted 14 September 2015 Published online 7 October 2015

Keywords 4H-SiC, heterojunctions, molecular beam epitaxy, p-type conductivity, thin films, ZnO

Stable p-type ZnO thin films on sapphire (0001) and n-type 4H-SiC (0001) substrates were achieved in low-ionized oxygen pressure using radical-source laser molecular beam epitaxy system. The p conduction type of ZnO films originates from not only zinc vacancy, but also interstitial oxygen acceptor defects, which was investigated by X-ray diffraction, atomic force microscopy, X-ray photoelectron spectroscopy, and photoluminescence measurements. The electrical properties were tested 180 days after deposition by Hall measurement. For the ZnO thin film grown on sapphire, a stable mobility of  $17.0\,\mathrm{cm^2\,V^{-1}s^{-1}}$ , a resistivity of  $1.08\,\Omega\mathrm{cm}$ , and a hole concentration of  $3.4\times10^{17}\,\mathrm{cm^{-3}}$  were achieved. The

selection of 4H-SiC substrates improved the crystalline quality of ZnO films confirmed by the X-ray diffraction patterns. An intrinsic p-type ZnO film on n-type 4H-SiC, with a stable mobility of  $44.6\,\mathrm{cm^2\,V^{-1}s^{-1}}$ , a resistivity of  $1.02\,\Omega\mathrm{cm}$ , and a hole concentration of  $1.4\times10^{17}\,\mathrm{cm^{-3}}$  were achieved. The current–voltage curve of the p–n ZnO homojunction shows typical diode characteristics, which also confirmed the achievement of the p-type ZnO. The current–voltage curve of the p-ZnO/n-4H-SiC heterojunction also shows p–n junction rectifier features. These results suggest the possibility of ultraviolet photodetectors and light-emitting devices.

© 2015 WILEY-VCH Verlag GmbH & Co. KGaA, Weinheim

**1 Introduction** Due to attractive electrical and optical properties, such as direct wide band gap (3.37 eV at RT) and high-exciton binding energy (60 meV at RT) [1], ZnO has gained much attention in various applications. Light-emitting diodes [2], photodetectors [3], and thin film transistors (TFT) [4] have been fabricated based on ZnO. One of the obstacles on the fabrication of high-performance device is the observation of the high-quality p-type ZnO thin films with significant hole carrier concentration. The compensation effect of native donor defects, such as oxygen vacancies and zinc interstitials is the main difficulty in achieving p-type conductivity [5, 6]. Recently, a number of groups have tried to address this issue by doping Group V

elements (N [7, 8], As [9], P [10], and Sb [11]), group I elements (Li [12] and Na [13]), and co-doping [14]. However, due to low solubility, high-activation energy, and poor crystal quality, the realization of p-type conductivity ZnO thin films for application is still an open question. More attention needs to be paid to improving the crystallinity of ZnO films and decreasing the background carrier concentration. There are a few reports on the growth of undoped p-type ZnO thin films in oxygen rich environment [15–18], and these reports lay the groundwork for the further study. The ZnO films were grown on sapphire or Si, and the lattice mismatches between ZnO thin films and these substrates were large, which may affect the crystallinity of ZnO films

<sup>&</sup>lt;sup>1</sup> Key Laboratory for Physical Electronics and Devices of the Ministry of Education and Key Laboratory of Photonics Technology for Information of Shaanxi Province, School of Electronics and Information Engineering, Xi'an Jiaotong University, Xi'an 710049, P.R. China

<sup>&</sup>lt;sup>2</sup> ISCAS-XJTU Joint Laboratory of Functional Materials and Devices for Informatics, School of Electronics and Information Engineering, Xi'an Jiaotong University, Xi'an 710049, P.R. China

<sup>\*</sup>Corresponding author: e-mail jwzhang@mail.xjtu.edu.cn, Phone/Fax: +86 29 8266 4684

18626319, 2016, 1, Downloaded from https://onlinelibrary.wiley.com/doi/10.1002/pssa.201532443 by CAS-XIAN INSTITUTION OPTICS PRECISION MECHANICS, Wiley Online Library on [10/11/2025]. See the Terms and Conditions (https://onlinelibrary.wiley.com/doi/10.1002/pssa.201532443 by CAS-XIAN INSTITUTION OPTICS PRECISION MECHANICS, Wiley Online Library on [10/11/2025]. See the Terms and Conditions (https://onlinelibrary.wiley.com/doi/10.1002/pssa.201532443 by CAS-XIAN INSTITUTION OPTICS PRECISION MECHANICS, Wiley Online Library on [10/11/2025]. See the Terms and Conditions (https://onlinelibrary.wiley.com/doi/10.1002/pssa.201532443 by CAS-XIAN INSTITUTION OPTICS PRECISION MECHANICS, Wiley Online Library on [10/11/2025]. See the Terms and Conditions (https://onlinelibrary.wiley.com/doi/10.1002/pssa.201532443 by CAS-XIAN INSTITUTION OPTICS PRECISION MECHANICS, Wiley Online Library on [10/11/2025]. See the Terms and Conditions (https://onlinelibrary.wiley.com/doi/10.1002/pssa.201532443 by CAS-XIAN INSTITUTION OPTICS PRECISION MECHANICS, Wiley Online Library on [10/11/2025]. See the Terms and Conditions (https://onlinelibrary.wiley.com/doi/10.1002/pssa.201532443 by CAS-XIAN INSTITUTION OPTICS PRECISION MECHANICS, Wiley Online Library on [10/11/2025]. See the Terms and Conditions (https://onlinelibrary.wiley.com/doi/10.1002/pssa.201532443 by CAS-XIAN INSTITUTION OPTICS PRECISION MECHANICS, Wiley Online Library on [10/11/2025]. See the Terms and Condition of the Condition of

onditions) on Wiley Online Library for rules of use; OA articles are governed by the applicable Creative Commons

to some extent. 4H-SiC, with the same wurtzite crystalline structure, is a good candidate for the growth of ZnO film. Moreover, 4H-SiC has only a 5% lattice mismatch to ZnO and the growth of ZnO thin film on it has no rotation of single cell [19]. There are a few reports on p-ZnO/n-6H-SiC [20, 21]; however, the studies on p-ZnO/n-4H-SiC were rarely reported.

In this work, we reported successful epitaxial growth of p- and n-type ZnO thin films on sapphire (0001) and 4H-SiC (0001) substrates by radical-source laser molecular beam epitaxy (RS-LMBE) system. We examined the effect of oxygen pressure on the conduction type of the ZnO films by comparing their crystallinity, optical properties, and carriers transport characteristics. The possible mechanism responsible for these results was analyzed. The current–voltage curves of the p–n ZnO homojunction and p-ZnO/n-4H-SiC heterojunction were displayed.

**2 Experimental** The ZnO films were grown on sapphire (0001) and n-type 4H-SiC (0001) by RS-LMBE system (Shenyang Scientific Instrument Co., Ltd., Chinese Academy of Sciences (SKY)). RS-LMBE uses a radiofrequency (RF) plasma source (Oxford Applied Research, HD-25) to ionize oxygen, and the oxygen plasma can not only suppress the background electron concentration but also reduce the formation energy of some acceptor defects, such as zinc vacancy [5, 22]. The 5N purity of ZnO target was vaporized by KrF excimer laser (Lambda Physik, Compex 102, 248 nm, 5 Hz, 100 mJ). The ground vacuum of the chamber was  $10^{-6}$  Pa. Before deposition, the sapphire and 4H-SiC substrates were cleaned with acetone and ethanol. Then, the sapphire substrates were treated in 3:1 solution of hot H<sub>2</sub>SO<sub>4</sub>:H<sub>3</sub>PO<sub>4</sub> (100 °C) for 10 min, while the 4H-SiC substrates were treated in 5% HF for 3 min. Finally the substrates were ultrasonic cleaned by de-ionized water for  $5\,\mathrm{min}$  and dried by high purity  $N_2$ . After being loaded into the vacuum chamber, the substrates were treated at 800 °C for half an hour. For the ZnO thin films grown on sapphire, a 10 nm low-temperature ZnO layer (LT-ZnO) was deposited at 300 °C, and then a 300 nm ZnO layer was deposited at 650 °C in the oxygen plasma. The oxygen (6N) pressure was from  $5 \times 10^{-4}$  to  $5 \times 10^{-3}$  Pa. The oxygen plasma was ionized by RF plasma source at 300 W. For the ZnO thin film grown on 4H-SiC, a 300 nm ZnO layer was directly deposited on the substrate without a LT-ZnO layer. The growth was under the same condition with the ZnO thin films grown on sapphire.

The photoluminescence (PL) spectra were carried out using a He-Cd laser with wavelength of 325 nm. The crystalline quality of the films was estimated by X-ray diffraction (XRD) (Philips X'Pert PW3040 high-resolution XRD system using  $CuK_{\alpha}$ ,  $\lambda=0.15406$  nm). The XRD measurement steps in this paper is  $0.001^{\circ}$ . The electrical properties were examined by Lake Shore 7707A Hall mobility system in a van der Pauw configuration with a magnetic field of 0.5 T. X-ray photoelectron spectroscopy (XPS) (PE, PHI-5400) was also used to analyze the origin of

the defects in the ZnO films. The samples have been etched by Ar<sup>+</sup> ion for 10 mins with a rate of 0.5 nm min<sup>-1</sup>. The surface morphography was studied by atomic force microscopy (AFM) (Veeco, Nano-Scope III).

**3 Results and discussion** Figure 1 shows the XRD  $2\theta$ - $\omega$  patterns of the ZnO thin films grown on sapphire (0001) and 4H-SiC (0001) substrates under various oxygen pressures. All the ZnO thin films show c-axis preferential growth. For ZnO thin films on Al<sub>2</sub>O<sub>3</sub> (0001) shown in Fig. 1(a), only strong ZnO (0002) and Al<sub>2</sub>O<sub>3</sub> (0006) peaks were observed at oxygen pressure lower than  $2 \times 10^{-3}$  Pa, which indicated good crystalline quality with hexagonal wurtzite structure. As the oxygen pressure increased up to  $5 \times 10^{-3}$  Pa, a weak extra peak at 33.027° appeared, which indicated a degradation of crystalline quality. The position of the (0002) diffraction peak ( $2\theta$ ) and the full width at half maximum (FWHM) (ω-rocking curves) and the average grain size (D) of the ZnO thin films were shown in Fig. 2. The average grain size (D) was estimated by the Scherrer equation [23]. As the oxygen pressure increased, the FWHM of the (0002) peaks decreased at  $1 \times 10^{-3}$  Pa and

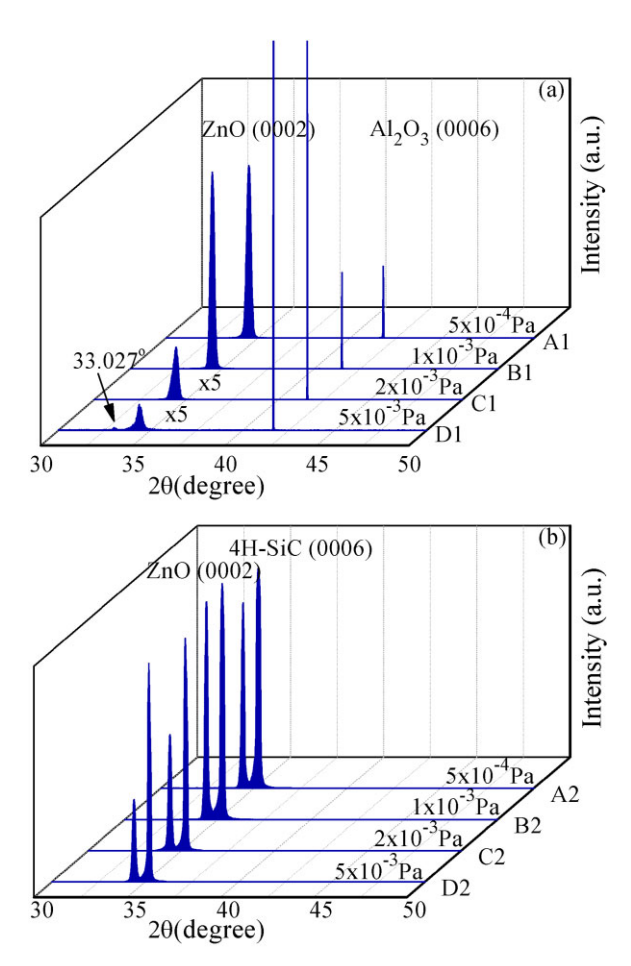


**Figure 1** XRD  $2\theta$ — $\omega$  patterns of the ZnO thin films on sapphire (0001) (a) and 4H-SiC (0001) substrates (b) under various oxygen pressures.

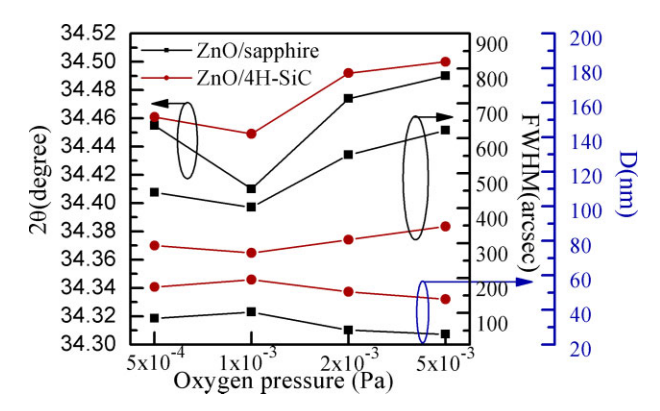


**Figure 2** The XRD position of the (0002) diffraction angle  $(2\theta)$ , the FWHM ( $\omega$ -rocking) and the average grain size (D) of the ZnO thin films on sapphire (solid squares) and 4H-SiC substrates (solid circles) under various oxygen pressures.

increased after that, while the average grain size (D) increased at  $1 \times 10^{-3}$  Pa, and decreased later. The oxygen pressure was also found to have quite an effect on the surface morphology as the AFM images shown in Fig. 3. The rms roughness of ZnO films grown on Al<sub>2</sub>O<sub>3</sub> was 3.37, 4.46, 2.59, and 1.37 nm, respectively. The grain size increased at  $1 \times 10^{-3}$  Pa, and then decreased after that, which was consistent with the calculated D. These results implied that moderate oxygen improved the crystalline quality, while excess oxygen might induce defects and resulted in the degradation of the crystalline quality. These results were similar to Ma's report [17].

It is well known that the diffraction (0002) peak position could be affected by the point defects (vacancy and

interstitial defects) and the residual strain induced by the lattice mismatch between ZnO and substrate. Under the oxygen pressure of  $5\times10^{-4}\,\mathrm{Pa}$ , the lack of oxygen-induced donor defects, such as oxygen vacancies (V<sub>O</sub>) and interstitial zinc (Zn<sub>i</sub>). If Zn<sub>i</sub> was dominant in the ZnO film, the Zn<sub>i</sub> usually located between O<sup>2-</sup> and Zn<sup>2+</sup> layers, and resulted in an increase of (0002) lattice spacing and a decrease of the diffraction angle (lower than 34.42° from a bulk ZnO) [24, 25]. In fact, the diffraction angle of the film grown at lowoxygen pressure was higher than 34.42°. It implied that the oxygen vacancies might be the most predominant defects in ZnO thin film at low-oxygen pressure, as V<sub>O</sub> can decrease the (0002) lattice spacing and increase the diffraction angle. At the oxygen pressure of  $1 \times 10^{-3}$  Pa, the vacancies were compensated by moderate oxygen to some extent, and combining with the residual strain, the diffraction angle decreased below 34.42°. It is noted that the oxygen plasma can enhance the oxygen chemical potential, which can lower the formation energy of some acceptor defects [5], such as the zinc vacancy (V<sub>Zn</sub>), the oxygen interstitial  $(O_i)$ , and the oxygen antisite  $(O_{Z_n})$ . The V<sub>Zn</sub> exhibited the lowest formation energy in all the range of the Fermi energy [6, 26]. As the oxygen pressure increased further, the excess oxygen might induce Zn vacancies, and the increased diffraction angle can be explained by the existence of the Zn vacancies [26, 27].

18626319, 2016. 1, Downloaded from https://onlinelibrary.wiley.com/doi/10.1002/psss.201532443 by CAS-XIAN INSTITUTION OPTICS PRECISION MECHANICS, Wiley Online Library on [10/11/2025]. See the Terms and Conditions (https://onlinelibrary.wiley.

onditions) on Wiley Online Library for rules of use; OA articles are governed by the applicable Creative Commons

For ZnO thin films grown on 4H-SiC (0001) substrates shown in Fig. 1(b), only ZnO (0002) and 4H-SiC (0006) existed, and the XRD results behaved similar to the ZnO films on sapphire substrates as the oxygen pressure increased. It can be seen that the FWHMs of the (0002) peaks for ZnO thin films grown on 4H-SiC substrates were

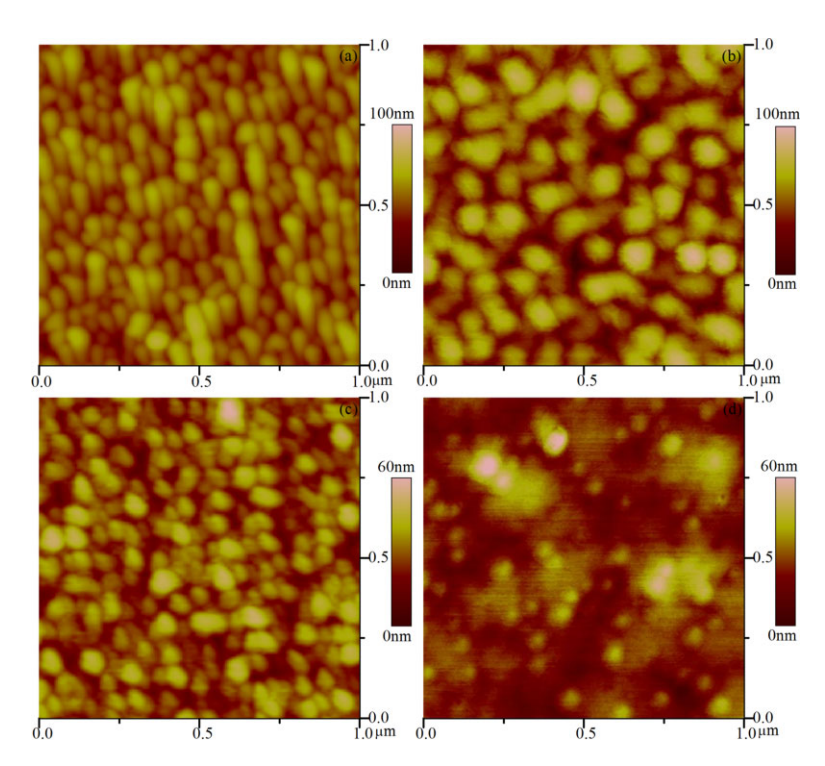


**Figure 3** The AFM images of the ZnO thin films on sapphire under various oxygen pressures. (a) Sample A1, (b) sample B1, (c) sample C1, and (d) sample D1.

**Table 1** The electrical properties of ZnO thin films grown on sapphire and 4H-SiC under various oxygen pressures measured by Hall effect measurement.

substrate	sample	oxygen plasma (10 <sup>-4</sup> Pa)	resistance (Ωcm)	concentration (cm <sup>-3</sup> )	$\begin{array}{c} \text{mobility} \\ (\text{cm}^2  \text{V}^{-1}  \text{s}^{-1}) \end{array}$	type
sapphire	A1	5	0.910	$1.0 \times 10^{17}$	66.8	n
	B1	10	_	_	_	n/p
	C1	20	0.153	$2.0 \times 10^{18}$	20.3	p
	D1	50	67.7	$1.3 \times 10^{17}$	0.690	p
4H-SiC	A2	5	_	_	_	n
	B2	10	_	_	_	n/p
	C2	20	0.150	$8.3 \times 10^{17}$	50.2	p
	D2	50	7.40	$9.5 \times 10^{16}$	8.91	p

smaller than ZnO films on sapphire as shown in Fig. 2. Moreover, the XRD pattern of the ZnO thin films grown on 4H-SiC substrates under  $5 \times 10^{-3}$  Pa did not exhibit other peaks besides (0002) peak (Fig. 1(b)). These facts implied that 4H-SiC substrates were more suitable for the nucleation of c-plane ZnO films than sapphire, owing to the small lattice mismatch between ZnO and 4H-SiC.

The oxygen pressure had quite an effect on the main electrical properties of ZnO thin films, which was confirmed by Hall measurement (Table 1). When the oxygen pressure was lower than  $5 \times 10^{-4}$  Pa,  $V_O$  was the main donor defect, and the ZnO thin films were characteristic of n-type conductivity with an electron concentration of  $1.0 \times 10^{17}$ cm<sup>-3</sup> (sample A1). The conductivity types of sample B1 and B2 were ambiguous, which suggested that the oxygen vacancies were compensated and there may be native acceptors formed competing with the native donors. The intrinsic p-type conductivity with a hole concentration above 10<sup>18</sup> cm<sup>-3</sup> had been achieved at the oxygen background pressure of  $2 \times 10^{-3}$  Pa. For further increase of oxygen pressure, the hole concentration and mobility decreased, while the resistance increased. This might be due to the formation of some complex defects involving the V<sub>Zn</sub>, the divacancy (V<sub>Zn</sub>V<sub>O</sub>), and the O-related defects in excess oxygen atmosphere. The complex defects either reduced the concentration of  $V_{Zn}$  or behaved as a deep donor to compensate the effect induced by  $V_{Zn}$  [28]. It can be seen from XRD patterns and AFM images that the samples grown on 4H-SiC substrates show larger grain size, which will result in less grain boundary area. As the formation energy of vacancies inside the grain was usually higher than that at the grain boundary, the V<sub>Zn</sub> concentration in sample C2 was lower than that in sample C1 and the hole concentration of sample C2 was lower than sample C1. The mobility of sample C2 was higher than C1, owing to the reduction of the scattering by lower native defects. The stability of the p-type ZnO samples (C1 and C2) was also investigated by Hall measurements 180 days after deposition, shown in Table 2. The conductivity type kept in p-type, and the hole concentrations were stable at  $\sim 10^{17} \, \text{cm}^{-1}$ 

XPS measurement was carried out to analyze the native defects of the n- and p-type ZnO films grown on sapphire

**Table 2** The electrical properties of the p-type ZnO samples (C1 and C2) measured by Hall effect measurement 180 days after deposition.

sample	resistance (Ωcm)	concentration (cm <sup>-3</sup> )	$\begin{array}{c} \text{mobility} \\ (\text{cm}^2\text{V}^{-1}\text{s}^{-1}) \end{array}$	type
C1	1.08	$3.4 \times 10^{17} \\ 1.4 \times 10^{17}$	17.0	p
C2	1.02		44.6	p

(sample A1 and C1), shown in Fig. 4. On the original surface of n-type ZnO film (sample A1, Fig. 4(a)), the individual O1s peak had been resolved into two components, positioned at around 530.3 and 531.5 eV, respectively. The component at the lower binding energy can be attributed to  $\rm O^{2-}$  ions on wurtzite structure of hexagonal  $\rm Zn^{2+}$  ion array ( $\rm O_L$ ); the higher binding energy component was due to O atoms in the oxygen deficient regions [29, 30], which indicated that the  $\rm V_O$  was attributed to the n-type conductivity and these results were in accordance with the XRD results. For the p-type ZnO film (sample C1, Fig. 4(b)), the O1s peak can only be resolved into two components, with the peak position at around 530.2 and

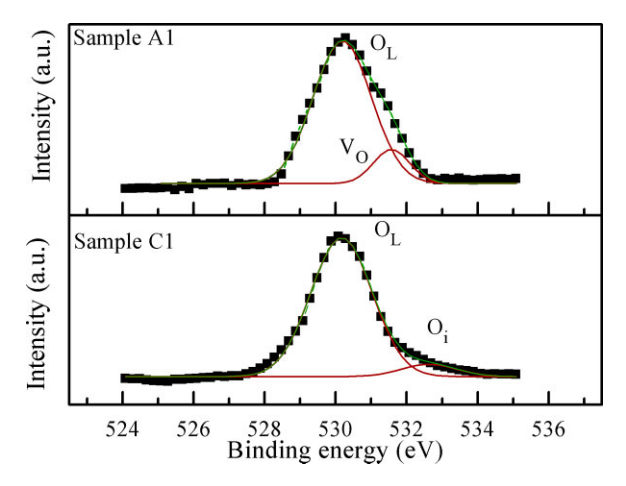


**Figure 4** XPS patterns of the n- and p-type ZnO films grown on sapphire (sample A1 and C1).



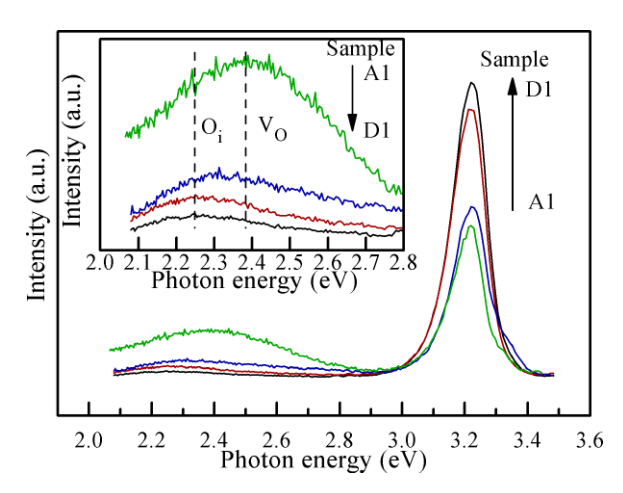
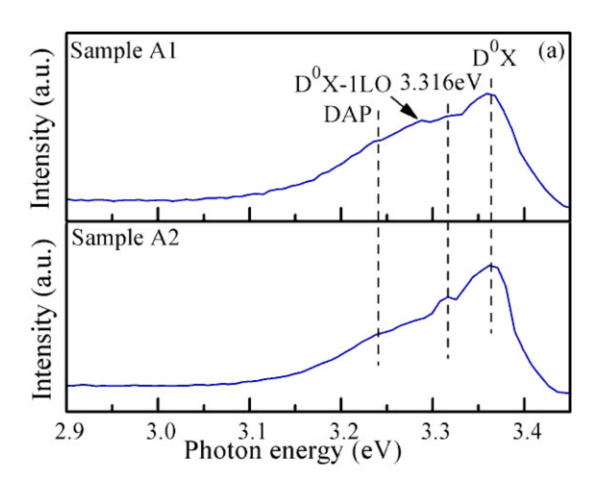


**Figure 5** The room temperature (RT) PL spectra of the ZnO films grown on sapphire under various oxygen pressures.

532.5 eV, respectively. The weak component appearing at the higher binding energy position corresponded to the interstitial O atoms (O<sub>i</sub>) or surface oxygen in forms of –OH groups [31]. As oxygen pressure increased, the  $V_{\rm O}$  decreased and finally the  $V_{\rm O}$ -related peak could not be seen in the O1s pattern, while an O<sub>i</sub> appear due to the excess oxygen. This result was somewhat different from the XRD analysis about  $V_{\rm Zn}$ . The only explanation was that both  $V_{\rm Zn}$  and O<sub>i</sub> were existed in the p-type ZnO thin film. As the O<sub>i</sub> peak was very weak, the  $V_{\rm Zn}$  was dominant and both of them contributed to the p-type conductivity.

The room temperature (RT) PL spectra of the ZnO films grown on sapphire are shown in Fig. 5. The near-band-edge (NBE) ultraviolet (UV) emission was at around 3.22 eV (385 nm), which was attributed to the combination of free exciton recombination [32]. As the oxygen pressure increased, the intensity of NBE increased. The green and yellow luminescence is shown in Fig. 5. The intensities of the green/yellow luminescence peaks decreased as the oxygen pressure increased, and the peak position shifted from  $\sim 2.37$  to  $\sim 2.25$  eV. The green luminescence (GL) at  $\sim 2.37 \,\text{eV}$  is ascribed to single-ionized  $V_O$  [33, 34]. The yellow luminescence (YL) at  $\sim$ 2.25 eV attributed to interstitial oxygen [35]. The results indicated that the concentration of Vo became lower and lower with more and more oxygen, which made the GL weaker and weaker. At the same time, the weak YL presented, which agreed with the XPS patterns. For the ZnO films grown on 4H-SiC, the variation trend of the RT PL spectra under various oxygen pressures was similar to Fig. 5, and their RT PL spectra are not shown in the present paper.

The low temperature (LT) (20 K) PL spectra of the n-(sample A1 and A2) and p-type (sample C1 and C2) ZnO thin films are shown in Fig. 6. For the n-type ZnO films (Fig. 6(a)), the prominent emission peak centered at 3.359 (sample A1) and 3.361 eV (sample A2) can be attributed to the recombination of excitons bound to neutral donors (D<sup>0</sup>X) [36–38]. The emission peak at around 3.25 eV was



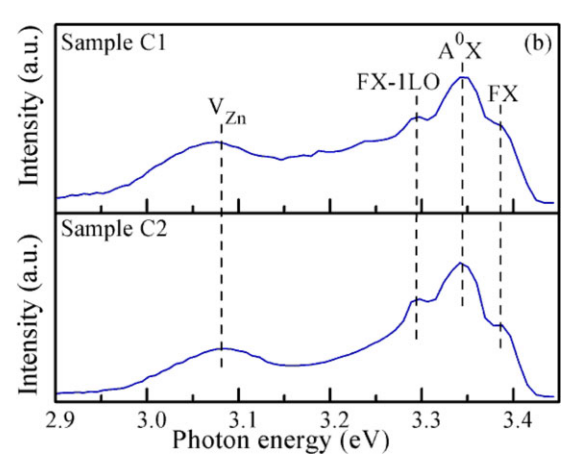


**Figure 6** The low temperature (20 K) PL spectra of the n-type (sample A1 and A2) (a) and p-type (sample C1 and C2) (b) ZnO thin films.

assigned to the recombination of donor-acceptor pair (DAP) [39]. The 3.287 eV of sample A1 was the first LO photon replica of  $D^0X$ . The 3.316 eV both existed in the two samples were unclear, and may relate to some DAP or twoelectron satellites of donor-bound excitons (TES-D<sup>0</sup>X). Figure 6(b) shows the LT-PL (20 K) spectra of p-type ZnO thin film (sample C1 and C2). The PL spectra was dominated by the neutral acceptor bound excition  $(A^0X)$ located at 3.339 and 3.336 eV. The 3.379 and 3.306 eV peaks were associated with free exciton (FX) and the first LO photon replica of the free exciton (FX-1LO). To determine the nature of defect-induced peak, the temperature dependence of PL peak was generally used. The temperature dependence of transition related to bound exciton follows the band gap energy variation according to Ref. [40]

$$E(T) = E_{g}(T) - E_{FX} - E_{l}, \tag{1}$$

where E(T) is the energy of the bound exciton,  $E_g(T)$  is the band gap energy [41],  $E_{FX}$  is the binding energy of FX, and

18626319, 2016, 1, Downloaded from https://onlinelibrary.wiley.com/doi/10.1092/pssa.201532443 by CAS-XIAN INSTITUTION OPTICS PRECISION MECHANICS, Wiley Online Library on [10/1/12/025]. See the Terms and Conditions (https://onlinelibrary.wiley.com/terms

-and-conditions) on Wiley Online Library for rules of use; OA articles are governed by the applicable Creative Commons

18026319, 2016, 1, Downloaded from https://onlinetibrary.wile.com/doi/10.1002/pss.20.153243 by CAS-XIAN INSTITUTION OPTICS PRECISION MECHANICS, Wiley Online Library on [10112025]. See the Terms and Conditions (https://onlinetibrary.wiley.com/terms-and-conditions) on Wiley Online Library or Included from https://onlinetibrary.wiley.com/terms-and-conditions) on Wiley Online Library or Included from https://onlinetibrary.wiley.com

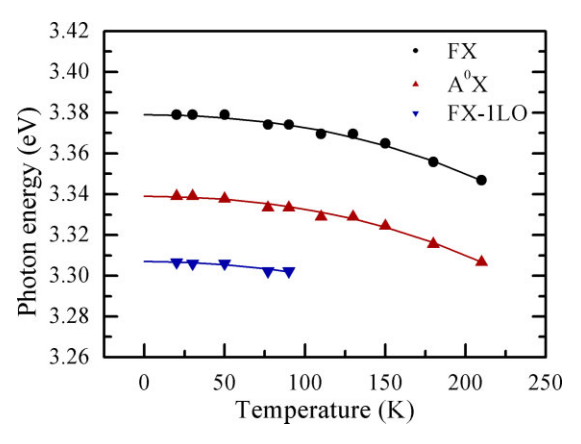


**Figure 7** Temperature-depended PL peak positions of the p-ZnO on sapphire.

the  $E_{\rm l}$  is the localization energy of the exciton on the defect. As shown in Fig. 7, the temperature dependence of FX, A<sup>0</sup>X and FX-1LO emission implied the exciton nature. The localization energy of A<sup>0</sup>X observed from the PL data was 40 meV ( $E_{\rm l} = E_{\rm g} - E_{\rm FX} - 3.339$ ). The binding energy of the defect is about 133 meV using Haynes rule  $E_{\rm l} = 0.3 E_{\rm def}$  [42, 43]. This result was consistent with the reported value (123 meV), which was related to the V<sup>0</sup><sub>Zn</sub> in ZnO [44].

There are several reports on  $V_{Zn}$ -related emission, such as 3.028 eV at 20 K [17], 3.1 eV at 80 K [45], and 3.09 eV at 6 K [46]. The emission peaks at 3.076 and 3.084 eV were considered as the transition of electron from conduction band to  $V_{Zn}$ . The intensity of this  $V_{Zn}$ -related peak of sample C2 was lower than that of sample C1, which indicated that the lower  $V_{Zn}$  concentration existed in the ZnO thin film on SiC substrates. The RT and LT PL spectra confirmed both  $V_{Zn}$  and  $O_i$  existed in the p-type ZnO thin film, and  $V_{Zn}$  was the main acceptor defect. The native defects behaved similar to the report of Lee et al. [47].

Figure 8 shows *I–V* characteristics of the n-ZnO/p-ZnO structure at room temperature. The n-type ZnO was

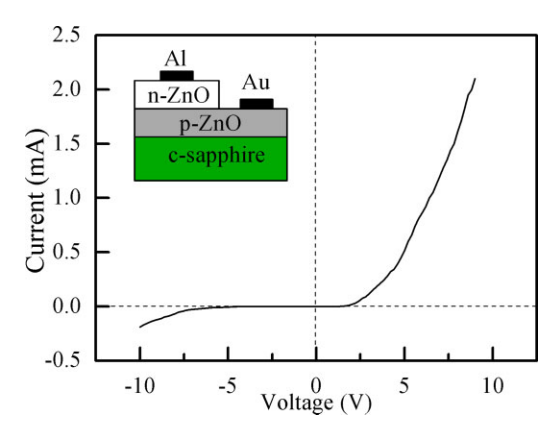


**Figure 8** *I–V* characteristics of the n-ZnO/p-ZnO structure. The inset shows the schematic diagram of the n-ZnO/p-ZnO/sapphire.

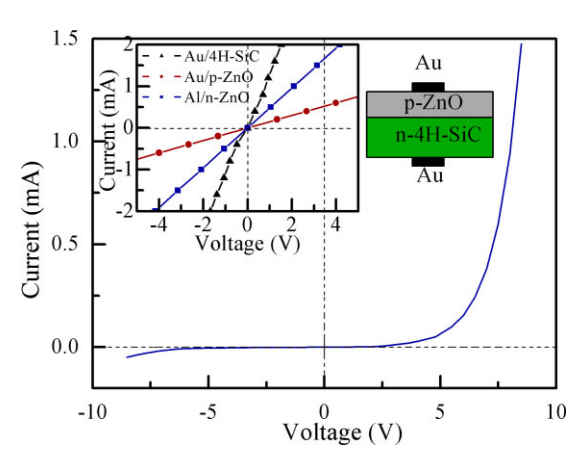


**Figure 9** *I–V* characteristics of the p-ZnO/n-4H-SiC heterojunction. The inset (left) shows the ohmic contacts on p-ZnO, n-ZnO and n-4H-SiC. The inset (right) shows the schematic diagram of the p-ZnO/n-4H-SiC.

deposited on the p-ZnO film without using the RF plasma source. The *I–V* curve shows the obvious p–n junction rectifier features. The turn-on voltage was about 3 V. The successfully produced p-ZnO/n-ZnO diode indicated the p-type conduction of ZnO was indeed achieved by controlling the oxygen pressure.

Figure 9 shows an *I–V* characteristic for p-ZnO/n-4H-SiC heterojunction. The turn-on voltage was larger than 5 V, which may be due to the formation of some very thin oxide such as Zn<sub>2</sub>SiO<sub>4</sub> [48] or some other reasons. Au was used as both p-ZnO and n-4H-SiC electrodes. Al was used as electrode on n-ZnO. The *I–V* curves of ohmic contacts on ZnO films are displayed in the inset of Fig. 9.

**4 Conclusions** In summary, the p-type ZnO thin films were realized by controlling the low ionized-oxygen pressure using RS-LMBE on sapphire (0001) and n-type 4H-SiC (0001). The ZnO film fabricated under the oxygen pressures larger than  $2 \times 10^{-3}$  Pa demonstrated p-type conductivity. The origin of the conversion of conduction type for ZnO films was confirmed by XRD, AFM, XPS, and PL measurements. The V<sub>O</sub> donor defects were dominant for the n-type film. The dominant  $V_{Zn}$  and secondary  $O_i$ acceptor defects were attributed to the p-type films. For the ZnO thin film grown on sapphire, an intrinsic p-type ZnO film with the high hole concentration of  $2.0 \times 10^{18} \, \text{cm}^{-3}$ was observed 3 days after deposition by Hall effect measurement, and then a stable mobility of  $17.0 \,\mathrm{cm}^2 \,\mathrm{V}^{-1} \mathrm{s}^{-1}$ , a resistivity of  $1.08\,\Omega\text{cm}$ , and a hole concentration of  $3.4 \times 10^{17} \,\mathrm{cm}^{-3}$  were achieved 180 days after deposition. The XRD patterns indicated the ZnO film on 4H-SiC had better crystalline quality. An intrinsic p-type ZnO film on n-type 4H-SiC, with a stable mobility of  $44.6 \,\mathrm{cm}^2 \,\mathrm{V}^{-1} \mathrm{s}^{-1}$ , a resistivity of  $1.02\,\Omega\text{cm}$ , and a hole concentration of  $1.4 \times 10^{17} \,\mathrm{cm}^{-3}$  was also achieved. The p-n ZnO homojunction shows typical diode characteristics. The turn-on voltage was about 3 V. The p-ZnO/n-4H-SiC heterojunction



also shows p—n junction rectifier features. However, the turn-on voltage was larger than 5 V, the further study on p-ZnO/n-4H-SiC heterojunction will be done in the future. This study lays the groundwork for further study of optoelectronic devices.

**Acknowledgements** This work was supported by Project 863 of the Ministry of Science and Technology of the People's Republic of China (2013AA03A101) and National Natural Science Foundation of China (nos. 60876042 and 61176018).

## References

- [1] Z. K. Tang, G. K. L. Wong, P. Yu, M. Kawasaki, A. Ohtomo, H. Koinuma, and Y. Segawa, Appl. Phys. Lett. 72, 3270 (1998).
- [2] S. He, C. X. Shan, J. S. Liu, B. H. Li, Z. Z. Zhang, and D. Z. Shen, Phys. Status Solidi B 250, 2102 (2013).
- [3] S. Y. Li, W. Tang, X. L. Xu, M. T. Cao, Y. Z. Jin, and X. J. Guo, Phys. Status Solidi A 211, 2184 (2014).
- [4] H. J. Jeon, S. G. Lee, K. S. Shin, S. W. Kim, and J. S. Park, J. Alloys. Compd. 614, 244 (2014).
- [5] S. B. Zhang and S. H. Wei, Phys. Rev. B 63, 075205 (2001).
- [6] F. Oba, S. Nishitani, S. Isotani, H. Adachi, and I. Tanaka, J. Appl. Phys. 90, 824 (2001).
- [7] D. Wang, J. W. Zhang, Y. P. Peng, Z. Bi, X. M. Bian, X. A. Zhang, and X. Hou, J. Alloys. Compd. 478, 325 (2009).
- [8] L. Li, C. X. Shan, B. H. Li, J. Y. Zhang, B. Yao, D. Z. Shen, X. W. Fan, and Y. M. Lu, J. Mater. Sci. 45, 4093 (2010).
- [9] C. K. To, B. Yang, S. C. Su, C. C. Ling, C. D. Beling, and S. Fung, J. Appl. Phys. 110, 113521 (2011).
- [10] Y. H. Xue, X. D. Zhang, Y. Y. Shen, D. C. Zhang, F. Zhu, L. H. Zhang, and C. L. Liu, Semicond. Sci. Technol. 26, 125016 (2011).
- [11] T. Yang, B. Yao, T. T. Zhao, G. Z. Xing, H. Wang, H. L. Pan, R. Deng, Y. R. Sui, L. L. Gao, H. Z. Wang, T. Wu, and D. Z. Shen, J. Alloys. Compd. 509, 5426 (2011).
- [12] B. Wang, L. D. Tang, J. G. Qi, H. L. Du, and Z. B. Zhang, J. Alloys. Compd. 503, 436 (2010).
- [13] S. S. Lin, Appl. Phys. Lett. 101, 122109 (2012).
- [14] Z. Yan, X. Zhang, Y. H. Liu, X. Y. Zhou, and J. Liang, J. Mater. Sci. 46, 2392 (2011).
- [15] Y. C. Huang, Z. Y. Li, L. W. Weng, W. Y. Uen, S. M. Lan, S. M. Liao, T. Y. Lin, Y. H. Huang, J. W. Chen, and T. N. Yang, J. Vac. Sci. Technol. A 28, 1307 (2010).
- [16] U. Ilyas, R. S. Rawat, T. L. Tan, P. Lee, R. Chen, H. D. Sun, F. J. Li, and S. Zhang, J. Appl. Phys. 110, 093522 (2011).
- [17] Y. Ma, G. T. Du, S. R. Yang, Z. T. Li, B. J. Zhao, X. T. Yang, T. P. Yang, Y. T. Zhang, and D. L. Liu, J. Appl. Phys. 95, 6268 (2004).
- [18] Ch. Pandis, N. Brilis, D. Tsamakis, H. A. Ali, S. Krishnamoorthy, and A. A. Iliadis, Solid-State Electron. 50, 1119 (2006).
- [19] Y. Clement, S. F. Yu, S. P. Lau, Rusli, and T. P. Chen, Appl. Phys. Lett. 86, 241111 (2005).
- [20] Z. F. Shi, X. C. Xia, W. Yin, S. K. Zhang, H. Wang, J. Wang, L. Zhao, X. Dong, B. L. Zhang, and G. T. Du, Appl. Phys. Lett. 100, 101112 (2012).
- [21] M. Dutta and D. Basak, Electrochem Solid-State Lett. 14, H389 (2011).

- [22] Y. J. Zeng, Z. Z. Ye, W. Z. Xu, J. G. Lu, H. P. He, L. P. Zhu, B. H. Zhao, Y. Che, and S. B. Zhang, Appl. Phys. Lett. 88, 262103 (2006).
- [23] T. M. Sabine and S. Hogg, Acta Crystallogr. B 25, 2254 (1969).
- [24] B. L. Zhu, X. Z. Zhao, S. Xu, F. H. Su, G. H. Li, X. G. Wu, J. Wu, R. Wu, and J. Liu, Jpn. J. Appl. Phys. 47, 2225 (2008).
- [25] G. Z. Xing, B. Yao, C. X. Cong, T. Yang, Y. P. Xie, B. H. Li, and D. Z. Shen, J. Alloys. Compd. 457, 36 (2008).
- [26] A. F. Kohan, G. Ceder, D. Morgan, and G. Van de Walle Chris, Phys. Rev. B 61, 15019 (2000).
- [27] J. P. Zhang, G. He, L. Q. Zhu, M. Liu, S. S. Pan, and L. D. Zhang, Appl. Surf. Sci. 253, 9414 (2007).
- [28] J. Zhong, A. H. Kitai, P. Mascher, and W. Puff, J. Electrochem. Soc. 140, 3644 (1993).
- [29] S. Major, S. Kumar, M. Bhatnagar, and K. L. Chopra, Appl. Phys. Lett. 49, 394 (1986).

18626319, 2016, 1, Downloaded from https://onlinelibrary.wiley.com/doi/10.1002/pssa.201532443 by CAS-XIAN INSTITUTION OPTICS PRECISION MECHANICS, Wiley Online Library on [1011/2025]. See the Terms and Conditions (https://onlinelibrary.wiley.com/doi/10.1002/pssa.201532443 by CAS-XIAN INSTITUTION OPTICS PRECISION MECHANICS, Wiley Online Library on [1011/2025]. See the Terms and Conditions (https://onlinelibrary.wiley.com/doi/10.1002/pssa.201532443 by CAS-XIAN INSTITUTION OPTICS PRECISION MECHANICS, Wiley Online Library on [1011/2025]. See the Terms and Conditions (https://onlinelibrary.wiley.com/doi/10.1002/pssa.201532443 by CAS-XIAN INSTITUTION OPTICS PRECISION MECHANICS, Wiley Online Library on [1011/2025]. See the Terms and Conditions (https://onlinelibrary.wiley.com/doi/10.1002/pssa.201532443 by CAS-XIAN INSTITUTION OPTICS PRECISION MECHANICS, Wiley Online Library on [1011/2025]. See the Terms and Conditions (https://onlinelibrary.wiley.com/doi/10.1002/pssa.201532443 by CAS-XIAN INSTITUTION OPTICS PRECISION MECHANICS, Wiley Online Library on [1011/2025]. See the Terms and Conditions (https://onlinelibrary.wiley.com/doi/10.1002/pssa.201532443 by CAS-XIAN INSTITUTION OPTICS PRECISION MECHANICS, Wiley Online Library on [1011/2025]. See the Terms and Conditions (https://onlinelibrary.wiley.com/doi/10.1002/pssa.201532443 by CAS-XIAN INSTITUTION OPTICS PRECISION MECHANICS, Wiley Online Library of the Terms of the Te

and-conditions) on Wiley Online Library for rules of use; OA articles are governed by the applicable Creative Common

- [30] H. T. Cao, Z. L. Pei, J. Gong, C. Sun, R. F. Huang, and L. S. Wen, J. Solid State Chem. 177, 1480 (2004).
- [31] T. P. Rao, M. C. S. Kumar, A. Safarulla, V. Ganesan, S. R. Barman, and C. Sanjeeviraja, Physica B 405, 2226 (2010).
- [32] W. I. Park and G. C. Yi, J. Electron. Mater. 30, L32 (2001).
- [33] E. J. Yun, H. S. Park, K. H. Lee, H. G. Nam, and M. Jung, J. Appl. Phys. 103, 073507 (2008).
- [34] D. H. Fan, Z. Y. Ning, and M. F. Jiang, Appl. Surf. Sci. 245, 414 (2005).
- [35] Y. J. Lin, C. L. Tsai, Y. M. Lu, and C. J. Liu, J. Appl. Phys. 99, 093501 (2006).
- [36] C. Boemare, T. Monteiro, M. J. Soares, J. G. Guilherme, and E. Alves, Physica B 985, 308 (2001).
- [37] A. Teke, Ü. Özgür, S. Doğan, X. Gu, H. Morkoç, B. Nemeth, J. Nause, and H. O. Everitt, Phys. Rev. B **70**, 195207 (2004).
- [38] D. C. Reynolds, D. C. Look, B. Jogai, C. W. Litton, T. C. Collins, W. Harsch, and G. Cantwell, Phys. Rev. B 57, 12151 (1998).
- [39] J. C. Li, B. Yao, Y. F. Li, Z. H. Ding, Y. Xu, L. G. Zhang, H. F. Zhao, and D. Z. Shen, J. Appl. Phys. 113, 193105 (2013).
- [40] D. Tainoff, B. Masenelli, P. Mélinon, A. Belsky, G. Ledoux, D. Amans, C. Dujardin, N. Fedorov, and P. Martin, Phys. Rev. B 81, 115304 (2010).
- [41] B. K. Meyer, H. Alves, D. M. Hofmann, W. Kriegseis, D. Forster, F. Bertram, J. Christen, A. Hoffmann, M. Straβburg, M. Dworzak, U. Haboeck, and A. V. Rodina, Phys. Status Solidi B 241, 231 (2004).
- [42] V. Sh., Yalishev, Y. S. Kim, X. L. Deng, B. H. Park, and S. H. U. Yuldashev, J. Appl. Phys. 112, 013528 (2012).
- [43] J. R. Haynes, Phys. Rev. Lett. 4, 361 (1960).
- [44] A. Travlos, N. Boukos, C. Chandrinou, H.-S. Kwack, and L. S. Dang, J Appl Phys. 106, 104307 (2009).
- [45] T. V. Butkhuzi, A. V. Bureyev, A. N. Georgobiani, N. P. Kekelidze, and T. G. Khulordava, J. Cryst. Growth 117, 366 (1992).
- [46] S. H. Jeong, B. S. Kim, and B. T. Lee, Appl. Phys. Lett. 82, 2625 (2003).
- [47] K. H. Lee, N. I. Cho, E. J. Yun, and H. G. Nam, Appl. Surf. Sci. 256, 4241 (2010).
- [48] R. Mu, A. Steigert, N. Y. Lin, R. Wilks, M. Bär, and Y. F. Zhang, J. Phys. D, Appl. Phys. 48, 305304 (2015).